iScience

CellPress
OPEN ACCESS

Article

Common features of aging fail to occur in *Drosophila* raised without a bacterial microbiome

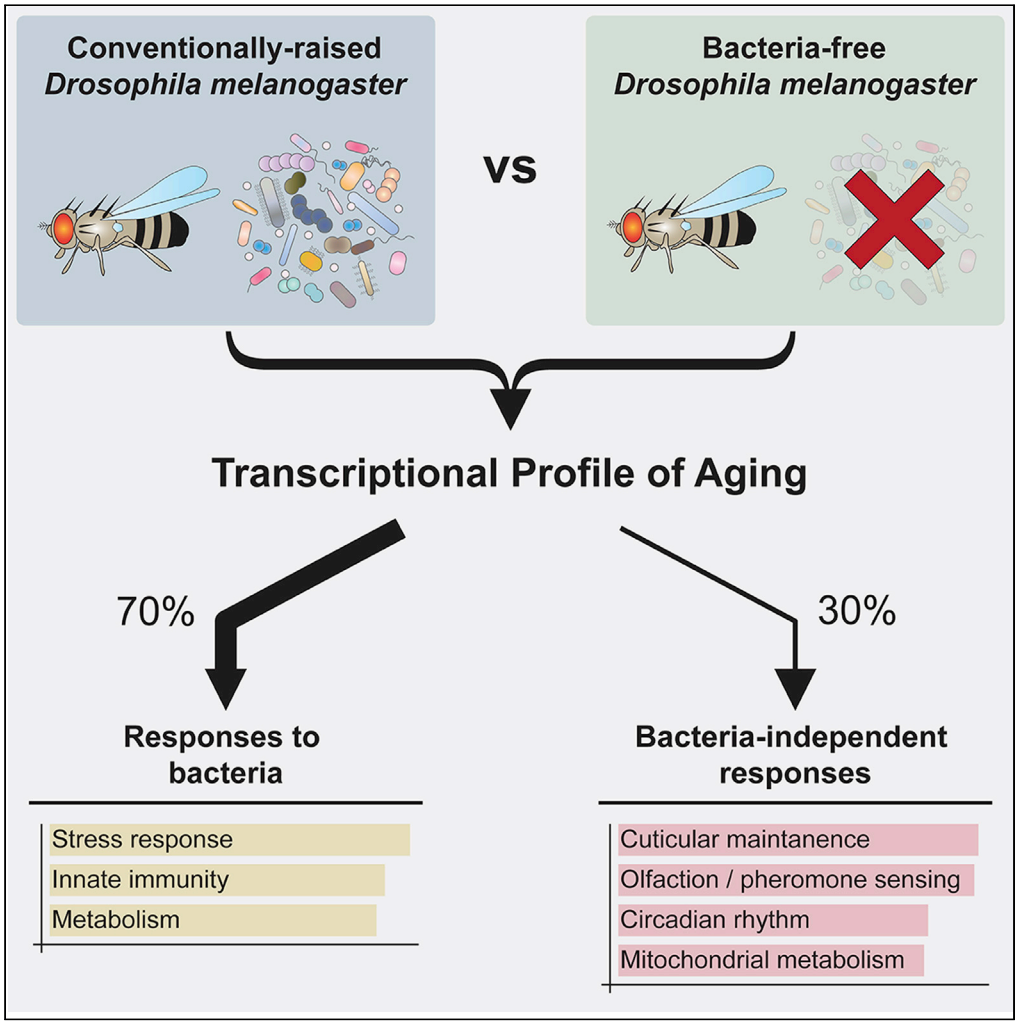

Arvind Kumar Shukla, Kory Johnson, Edward Giniger

ginigere@nih.gov

Highlights

70% of the changes in gene expression during aging are responses to the microbiome

Some of the most common features of aging never occur in flies that are germ-free

Stress response, immunity, and most metabolic changes are microbiome-dependent

Microbiome-independent features of aging can serve as biomarkers of age

Shukla et al., iScience *24*, 102703
July 23, 2021
https://doi.org/10.1016/j.isci.2021.102703

iScience

CellPress
OPEN ACCESS

Article

Common features of aging fail to occur in *Drosophila* raised without a bacterial microbiome

Arvind Kumar Shukla,[1] Kory Johnson,[1] and Edward Giniger[1,2,*]

SUMMARY

Lifespan is limited both by intrinsic decline in vigor with age and by accumulation of external insults. There exists a general picture of the deficits of aging, one that is reflected in a pattern of age-correlated changes in gene expression conserved across species. Here, however, by comparing gene expression profiling of *Drosophila* raised either conventionally, or free of bacteria, we show that ~70% of these conserved, age-associated changes in gene expression fail to occur in germ-free flies. Among the processes that fail to show time-dependent change under germ-free conditions are two aging features that are observed across phylogeny, declining expression of stress response genes and increasing expression of innate immune genes. These comprise adaptive strategies the organism uses to respond to bacteria, rather than being inevitable components of age-dependent decline. Changes in other processes are independent of the microbiome and can serve as autonomous markers of aging of the individual.

INTRODUCTION

Aging is the progressive decline in vigor and resilience suffered by an individual with the passage of time during adulthood. The progression of time-dependent deficits in an animal is conserved broadly across evolution (Pitt and Kaeberlein, 2015). These include deterioration in stress resistance (Dues et al., 2016), waning in the efficacy of proteostasis and autophagy (Hipp et al., 2019; Rubinsztein et al., 2011) with concomitant accumulation of defective proteins and lipids (Richardson and Schadt, 2014), and increase in the expression of cytotoxic effectors of the innate immune response (Zerofsky et al., 2005), among other features. This conserved pattern of age-dependent physiological changes is reflected in a pattern of change in gene expression that also is conserved across animal phylogeny (Fushan et al., 2015; Komljenovic A et al., 2019). It is widely thought that the decline in vitality with aging arises from the accumulation of time-dependent insults to the components of the cell–oxidative damage, radiation damage, alterations of DNA sequence–together with progressive decline in the efficacy of many aspects of cellular homeostasis and repair (Fraga et al., 1990; Hipp et al., 2019; López-Otín et al., 2013; Rubinsztein et al., 2011; Vijg and Montagna, 2017). Operationally, aging is typically viewed through two, complementary lenses. The increase of mortality in a population over time is often understood as reflecting the summed effects of a constellation of separate processes that act in parallel to progressively reduce the vigor of the individual (Pletcher et al., 2000; Stroustrup et al., 2016). Alternatively, it has been speculated that "age" can be represented as an internal state of the animal that integrates those time-dependent factors to define an autonomous measure of viability and vigor (Guarente and Kenyon, 2000; Tabula Muris, 2020) though such a view is open to evolutionary critique (Kirkwood and Melov, 2011). From either perspective, however, it is commonly accepted that aging is characterized by a collection of common features, or "hallmarks" (López-Otín et al., 2013) that are conserved through animal evolution, and that are obligatory components of the constellation of deficits we recognize as aging.

Commensal microbes provide another critical contribution to aging (Clark et al., 2015; Gould et al., 2018; Pryor et al., 2019; Smith et al., 2017). *Caenorhabditis elegans* grown without a bacterial microbiome (axenic) live twice as long as those grown conventionally (Houthoofd et al., 2002). Similarly, most analyses have suggested that *Drosophila* lifespan is extended by axenic growth (Clark et al., 2015; Galenza et al., 2016; Lee et al., 2019; Petkau et al., 2014), though that relationship depends on both growth conditions and the details of how such studies are performed (Brummel et al., 2004; Yamada et al., 2015). For example, lack of a

[1]National Institutes of Health, National Institute of Neurological Disorders and Stroke, Bldg 35, Rm 1C 1002, Bethesda, MD 20892, USA

[2]Lead contact

*Correspondence: ginigere@nih.gov

https://doi.org/10.1016/j.isci.2021.102703

microbiome, particularly early in life, may limit the development of a robust innate immune response and alter the expression of stress-response genes (Broderick et al., 2014), and therefore sensitize an individual to later microbial challenge (Belkaid and Hand, 2014). Moreover, the presence of a microbiome can compensate for a diet with low protein content, perhaps because the bacteria themselves act as a food source (Storelli et al., 2011). Multiple mechanisms, therefore, contribute to the modulation of lifespan in axenic conditions (Clark and Walker, 2018; Guo et al., 2014; Ren et al., 2007). Additionally, some studies link the microbiome-dependence of lifespan to specific commensal species, or to the interaction of specific commensals with variants in the host genome or compounds in the environment (Gould et al., 2018). For example, in *C. elegans*, at least some of the linkage between the microbiome and aging seems to be mediated by specific microbially-secreted metabolites (Han et al., 2017). Such specificity, however, is difficult to understand in light of the generality of the phenomenon, given the variety of experimental paradigms in which it has been observed.

Here, we perform genome-wide gene expression profiling of *Drosophila* raised either under conventional growth conditions or under axenic conditions. We find that approximately 70% of the systematic changes in gene expression that we observe with age under conventional conditions fail to happen when we grow the flies axenically. In essence, many of the typical correlates of *Drosophila* aging become uncoupled from the passage of time for the greater part of adulthood if the flies lack a bacterial microbiome. Among the genes that do not show expected, time-dependent changes in expression when flies are raised axenically are those associated with two features of aging that are observed widely across animal evolution, a decline in the expression of stress-resistance genes and progressive activation of innate immunity, as well as others. Thus, while these processes are clearly critical regulators of organismal lifespan, our data suggest that they are separable from other aspects of the typical progression of age-associated changes in organismal gene expression. They seem, rather, to reflect a succession of strategies that the organism has evolved for different stages of its lifecycle in order to exist in a microbe-rich environment. In contrast, genes associated with some age-correlated processes, including rhythmic behavior, maintenance of cuticular structure, olfaction, and a subset of metabolic and redox processes, show changes in level over time in the axenic state that are similar to those observed under conventional conditions, allowing us to use them as biomarkers to quantify the age-correlated physiological state of the germ-free animal. The experiments reported here, therefore, support the view that the organism is subject to a progression of separable processes that individually modulate organismal longevity, while also identifying biomarkers of a time-dependent, internal state of the animal that reflects its effective age.

RESULTS

Absence of a bacterial microbiome extends *Drosophila* lifespan

Motivated by experiments we have performed recently investigating the role of innate immunity in neurodegeneration (Shukla et al., 2019), we set out to measure the lifespan and aspects of gene expression in wild type flies that lack a bacterial microbiome due to chronic (multi-generation) growth in media containing antibiotics (Shukla et al., 2019). Consistent with most previous studies (Clark et al., 2015; Lee et al., 2019), axenic flies survived longer (Figure 1A, $p < 0.0001$; Logrank (Mantel-Cox) test); Table S1), with a median survival of 63.9 $\pm$ 0.9 days, while the median survival for conventionally raised flies was 57.5 $\pm$ 0.5 days (Figure1B, $p = 0.0308$). The absence of bacterial contamination of the axenic cultures was verified both by plating fly extract on multiple bacterial growth media and by PCR for 16S rDNA using universal bacterial probe sets (Figure S1). Plating extract on fungal media (YPD) revealed, first, that the load of fungal CFU was only ~1.0% of the bacterial load under conventional conditions, and second, that the fungal density was not changed when bacterial growth was suppressed with antibiotics (Figure S2).

To better understand the mechanism by which axenic growth extends lifespan, we applied a method we have described previously that uses genome-wide expression profiling to develop a set of biomarkers that quantify the "effective age", as opposed to the chronological age, of a fly population by capturing the time-dependent internal state of the fly's physiology (Spurrier et al., 2018). In essence, this method measures the systematic changes in the pattern of gene expression that occur over the lifespan and uses them as a standard curve, to which we compare the expression profile of an experimental sample to ask what chronological age it most closely resembles. In brief, RNA from heads of conventionally raised or axenic male flies was isolated at various ages (3, 10, 30, and 45 days), and the genome-wide RNA expression profile was quantified using microarrays. Next, a machine learning algorithm (k-nearest neighbor, with leave-one-out cross-validation) was used to identify aging "classifier genes", that is, genes whose

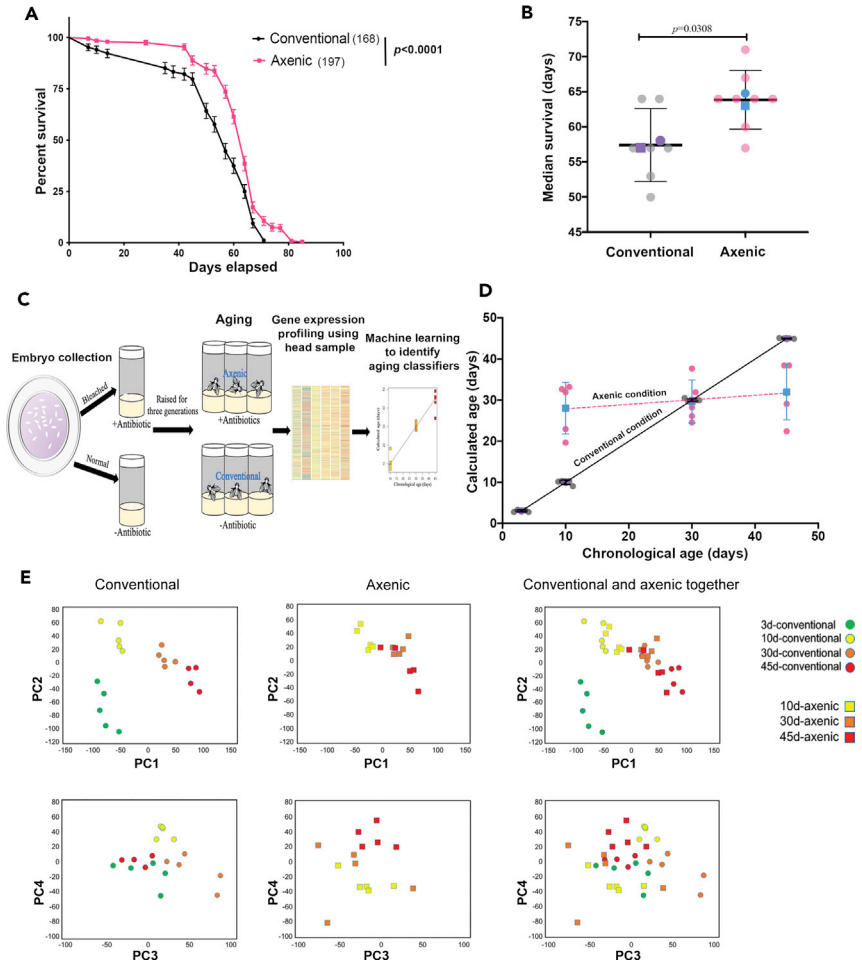

Figure 1. The absence of a microbiome affects lifespan and aging

(A) The percent surviving flies was plotted versus age in days for mated males that were raised conventionally (black curve) or axenic (red curve). Values plotted are mean ± SEM; pvalue calculated using Logrank (Mantel-Cox) test; starting number of flies is in parentheses. Data were pooled from two biological replicates, consisting of 3 or 4 technical replicates, respectively.

(B) Median lifespan for the two conditions presented as Mean ± SD. Median survival from individual technical replicates is shown in gray and red, respectively. Purple circle and square represent means of the two biological replicates for conventional flies; blue circle and square represent means of the two biological replicates for axenic flies. Signficance by Mann-Whitney test.

(C) Experimental design for generating the gene expression age metric.

(D) A linear model for transcriptomic age (calculated age) was developed using gene expression profiling data of conventionally raised flies and was used to calculate the effective age of axenic flies (details in STAR Methods; 5 biological replicates for all conditions). Conventional samples: replicates are gray circles; mean value is purple circle; SD is indicated. Axenic samples, replicates are red circles; mean value is blue square; SD is indicated. The black line is the regression line for calculated vs chronological age for conventionally-raised samples; the dashed red line is the regression line for axenic samples.

(E) Principal component analysis (PCA) plot for the overall structure of the data. PCA based on all genes is plotted with respect to first and second principal components (top graphs) or third and fourth principal components (bottom graphs). Green, yellow, orange, and red circles represent conventional samples and yellow, orange, and red squares denote axenic samples of the indicated ages.

See also Figures S1–S3.

expression level in conventionally raised flies can be used to predict their age with strong statistical support (Figure 1C). This selected 1628 out of the 15,034 significantly expressed genes (Table S2). The expression levels of these classifiers were then used to generate a linear model for calculated age (Figure 1D) (Spurrier

et al., 2018). Finally, we applied this linear model derived from the conventionally raised flies to gene expression data of axenically grown flies. We performed the age calculation only on 10-to 45-day-old axenic flies since flies younger than 10 days are physiologically immature and display a distinct and rapidly changing gene expression profile, while beyond 45 days large numbers of flies begin to die, again complicating the interpretation of gene expression data. Note that to control experimental variance, we limited our analysis to one sex (male), and further that we restricted our analysis to RNA from the head, which is dominated by neural tissue, though with contributions from epithelia and fat body, among others.

To our surprise, we found that throughout mature adulthood, from 10-45 days after eclosion, axenic flies displayed a genome-wide gene expression profile essentially equivalent to that of 30-day old conventionally raised flies. Thus, 10-day-old axenic flies measured 28.0 $\pm$ 2.8 days effective age; 30-day-old axenic measured 29.7 $\pm$ 2.3 days; and 45-day-old axenic measured 32.0 $\pm$ 3.0 days (mean $\pm$ SEM). We wondered whether the apparent convergence between the calculated ages for the 30-day-old conventional and 30-day-old axenic conditions was a faithful reflection of similarity in the underlying gene expression profiles at this age or just statistical happenstance. We, therefore, compared these two conditions directly by ANOVA and found that, indeed, only 64 genes (0.4% of genes queried) showed a significant difference in expression (Table S3; corrected $p < 0.05$; $\geq$1.5x change in expression level, out of 14,688 genes suitable for this comparison). We excluded the possibility that the failure to observe a progressive increase in calculated age over adulthood in axenic conditions was an artifact of high, nonspecific variance in gene expression by quantifying the coefficient of variation for all genes analyzed and finding that it was consistent under all experimental conditions tested (Figure S3).

To characterize further the overall structure of the data we next performed principal component analysis (PCA) (Figure 1E). First, this confirmed that the replicates of each experimental condition clustered in gene expression space. Moreover, those clusters separated by PC in ways consistent with the experimental design. Thus, for example, clusters corresponding to 3, 10, 30, and 45-d conventionally raised flies distributed smoothly along PC1, suggesting that this axis captures properties of aging, while PC3 largely (though not perfectly) separated the conventional samples from the axenic samples. Remarkably, and in contrast to the conventional samples, the 10, 30 and 45-d axenic samples were relatively clustered along PC1 and not distributed, consistent with the apparent compression of gene expression age under axenic conditions revealed by the machine learning analysis above.

We next investigated whether the properties of the expression profile in the axenic state might be driven by the presence of antibiotics rather than by the absence of bacteria. This seemed unlikely, both because the antibiotic regimen used here has been characterized extensively in previous studies (Koyle et al., 2016; Leftwich et al., 2017; Schneider et al., 2019) and because of the failure to detect xenobiotic response as a major gene ontology (GO) category among genes with significantly altered expression (see below). Nonetheless, we performed two experimental tests that argue strongly against this hypothesis. First, we raised axenic flies for 5 d on antibiotic-containing food to ensure microbial sterility, and then shifted the flies for an additional 5 d to antibiotic-free food before performing qPCR to quantify the expression of genes whose level we had previously found to differ between conventional vs axenic conditions at 10 d. We found that in 8 out of 8 cases of genes whose expression differed between conventional vs antibiotic growth conditions, withdrawing the antibiotic did not restore the conventional level of expression (Figure 2). In contrast, if removal of antibiotic was accompanied by reintroducing normal *Drosophila* flora (by culturing the flies in vials that had previously been used to house non-axenic flies) all 8 of those genes did show restoration of gene expression toward the conventional pattern. As a second test, we derived new axenic flies acutely, by bleaching eggs from conventionally raised flies to sterilize them. We then raised the resulting adults either in clean vials, without ever exposing them to antibiotics, or in vials that had been pre-equilibrated with the normal lab flora, and performed qPCR on the same genes investigated in Figure 2A, above, again using RNA from 10-day-old adults. All genes analyzed showed low levels of expression in the acutely axenic (no-antibiotic) state, consistent with their expression in the presence of antibiotics. Upon reintroduction of bacteria, in contrast, all but one showed substantially increased expression, again as in our previous, microbe-rich conditions (Figure S4). Thus, in both experimental tests, the axenic pattern of gene expression correlated with the presence or absence of bacterial flora, and not with the presence of antibiotics.

Taken together, these data show that while growth under axenic conditions modestly increases the lifespan of the fly, its far more profound effect was to grossly change the relationship between genome-wide gene expression and chronological age across the adult lifespan.

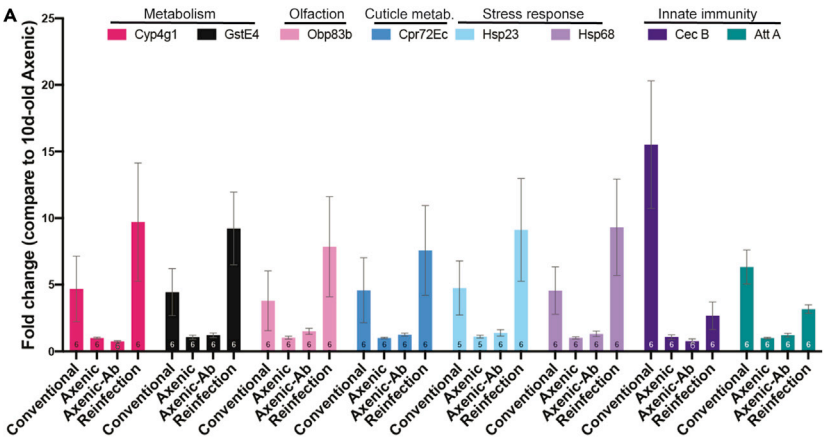

B

Measure of variance	Conventional	Axenic	% reduction in axenic
Number of aging classifier genes, based on machine learning analysis	869	189	78
Variance accounted for by aging, based on PCA of classifier genes (SD)	41.1	11.7	72
Number of age-correlated genes, based on polyserial analysis	4577	930	80
Variance accounted for by aging, based on PCA of polyserial-selected genes (SD)	69.7	26.3	62
Number of genes with significantly altered expression (10d vs 45d; ANOVA)	954	275	71

Figure 2. Quantification of the effect of antibiotics and of the age-correlated variance in conventional and axenic conditions

(A) Eight representative genes were selected for qPCR validation from among five biological processes (metabolism, olfaction, cuticle, stress response, and immunity, as indicated). Fold change was calculated compared to 10-day-old axenic sample after normalization with Rpl32. Bars represent mean ± SEM; number of replicates is shown at the bottom of each bar. Conventional: Flies raised for 10d in conventional food; Axenic: Flies raised in food with antibiotic supplementation for 10 d; Axenic-Ab: 5-day-old axenic flies transferred to sterile food without antibiotics and raised for an additional five days; Reinfection: 5-day-old axenic flies transferred to vials previously used for growing conventional flies and raised an additional five days.

(B) Different methods of calculating age-correlated variance in gene expression, as indicated, were applied separately to the data from conventionally raised and axenic flies and compared.

See also Figures S1–S3.

Approximately 70% of the gene expression changes observed during aging under conventional conditions do not occur in axenic flies

While investigating the properties of aging classifier genes above, we noticed that selecting classifiers from axenic 10-, 30- and 45-day samples identified only 189 classifier genes, 78% fewer than the number of classifiers identified by applying the same procedure to data from 10-, 30- and 45-day conventionally raised flies (869 genes). Since we had already shown that there is no significant difference in the amount of random noise in the conventional vs axenic datasets (Figure S3, above), this seemed to suggest a selective reduction in age-dependent changes in gene expression in the axenic state. To test this interpretation, we used four additional methods to compare the age-correlated variation in gene expression under the two sets of growth conditions (Figure 2B). First, we used PCA to quantify the variance accounted for by age within the two sets of classifier genes and found that it was reduced 72% in the axenic set (11.7 SD, vs 41.1 for conventional). Next, we used an unrelated method to identify age-correlated genes and repeated these analyses. Specifically, we performed polyserial correlation analysis of the expression level of each gene vs age (10-, 30- and 45-day) in conventionally grown and axenic flies. After correcting for multiple testing, we found that the number of genes with age-correlated expression was reduced by 80% in the axenic condition (930, vs 4577 in conventional; Table S4), and the variation explained by age, as calculated by PCA, was decreased by 62% (SD 26.3 vs 69.7 in conventional). Finally, we also performed ANOVA to determine directly how many genes showed significantly altered expression in a comparison of 45-day- vs 10-day-old samples in each condition. Again, the axenic condition produced a 71% decrease in the number of significantly altered genes relative to conventionally -grown flies (275 genes with an altered expression between the two ages in the axenic samples, vs 954 in the conventional; Table S5). The decrease in the number of gene differences identified by ANOVA in the axenic condition was not merely a consequence of the statistical cutoff, as we

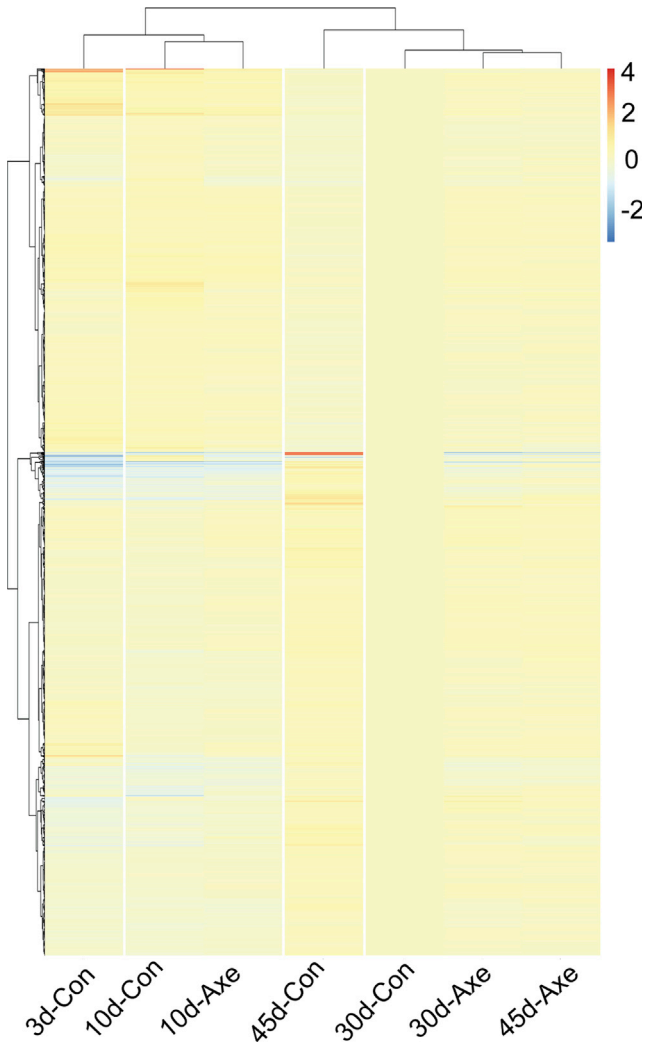

Figure 3. Heatmap of relative expression of age-correlated genes

Relative expression of all genes selected as age-correlated based on polyserial correlation under conventional conditions is displayed as a heatmap across all conditions. Sample-level fold change (log_2) was calculated using the mean value for each gene in each condition, relative to the 30-d conventional condition. Data is presented organized by unsupervised clustering (pheatmap). Experimental condition is indicated at the bottom of each column; Y-axis represents 4577 genes. Color key for fold-change is shown at the upper right.

See also Figures S5 and S6.

also observed a 66% drop in the number of genes selected using a $\pm$1.5 fold change cutoff irrespective of the pvalue (341 genes with an altered expression between the two ages for axenic samples vs 1018 in the conventional; Table S6). Together, these analyses confirm that age-dependent variation in gene expression is massively reduced in flies raised under axenic conditions.

The apparent reduction of age-dependent change in gene expression under axenic conditions was entirely unexpected. We, therefore, visualized the global pattern of gene expression by selecting all genes whose expression is age-correlated under conventional conditions (by polyserial correlation; 4577 genes out of 15,034 significantly expressed genes total) and displaying their expression under all experimental conditions as a heatmap, using expression level in 30d conventionally raised flies as the baseline (Figure 3; for heatmap of individual samples see Figure S5; annotated heatmap data values, Table S7. The same heatmap is presented with different color coding in Figure S6 to enhance discrimination of subtle differences). Based both on visual inspection of the heatmap and the results of unsupervised clustering (pheatmap) the global gene expression pattern was consistent with predictions from the PCA and machine learning

analyses. Thus, for example, the 30d axenic condition clustered most closely to the 30d conventional condition. Moreover, clear similarities were apparent in the overall pattern of gene expression among all three axenic conditions (10, 30, and 45 d). It is also apparent that the 10d and 45d conventional conditions show distinct differences from 30d conventional, particularly among up-regulated genes that are not observed in axenic samples of the same ages. Finally, also as expected, the 3d conventional sample separated from all other conditions.

We next used GO analysis to compare the pattern of age-dependent gene expression changes observed under conventional vs axenic growth, and found that many conserved features of the collection of age-dependent changes one typically observes under conventional conditions fail to occur when flies are grown in the absence of their usual bacterial flora. We applied the GO package DAVID (Database for Annotation, Visualization and Integrated Discovery, v. 6.8) (Huang et al., 2009a, 2009b) to the set of aging classifier genes from conventionally raised flies (Figure 4A, Table S8) to identify biological processes whose representation was significantly enriched (Figure 4B, Table S9). For this analysis, classifier selection was restricted to data from 10-, 30-, and 45-day samples to facilitate comparison with axenic conditions. To simplify visualization, we have presented the data with enriched processes sorted manually into groups based on function and arranged each group by the degree of enrichment (Figure 4B). GO analysis of the gene expression profile of flies grown in conventional conditions revealed five major categories of biological processes: Immunity, Olfaction/Sensation, Stress Response, Rhythmic Behavior, and Metabolism, similar to findings of previous studies by us and others (Pacifico et al., 2018; Pletcher et al., 2002; Spurrier et al., 2018). We then performed DAVID analysis on aging classifiers derived the same way from the axenic expression profiles (Table S8). In contrast to the conventionally grown flies, in axenic flies two central categories of biological processes that are commonly viewed as "hallmarks of aging" (López-Otín et al., 2013), Stress Response and Innate Immunity, are largely or entirely absent from the list of enriched GO terms. Examination of expression levels reveals that whereas 10-d conventionally grown flies have substantially elevated expression of stress response genes, for example, Hsp70, Hsp26, and Hsp27, as compared with 30-d conventionally grown flies, 10-d axenic flies fail to activate most of those stress genes (Figure 4C, Table S10; a complete listing of genes included in each GO category is given in Table S11). Similarly, at 45 d, axenic flies fail to activate the expression of genes of the innate immune response, such as CecC, DptB, and AttA, as opposed to their high-level expression in conventionally grown flies (Figure 4D, Table S10). In addition to these two categories, a diverse selection of normally age-dependent genes classified by DAVID as being associated with Metabolism fail to show age-dependent modulation of expression under axenic conditions (Figure 4B; Table S9). This category was too large and complex for us to discern any simple theme among its constituents, and it includes both genes that fail to show up-regulation with increasing age and others that fail to show down-regulation. These GO results accord well with a previous expression profiling analysis of dissected gut from conventionally raised vs axenic *Drosophila*, which also reports significant microbiome-dependent changes in expression of genes related to immunity, stress response, and aspects of metabolism (though that experiment also detected changes in cell differentiation genes likely associated specifically with gut homeostasis) (Broderick et al., 2014). Similarly, gene expression comparison of conventional vs germ-free tissue from mouse brain reported large effects in particular on genes related to immune function (as well as myelination, a property we cannot asssess in the fly) (Hoban et al., 2016). In contrast to the three GO categories that are absent from axenic flies, some processes remain enriched among age-dependent processes in both conventional and axenic conditions, including rhythmic behavior (e.g., circadian rhythm, locomotor rhythm), chitin-based cuticle development, and sensory perception of smell (Figure 4B; Table S9). To confirm these observations, we used qPCR to validate the expression of 10 representative genes selected from among different enriched biological processes (circadian rhythm, metabolism, cuticle, immunity, olfaction, and stress response) and found 100% concordance with the array results (Figure S7). Thus, the majority of the consistent changes in gene expression that normally occur with age fail to happen when flies are raised in the absence of bacteria, including some generally accepted hallmarks of the aging process.

Axenic growth reduces aging rate only modestly as quantified with transcriptional biomarkers

Since a large fraction of the genes we used for the initial assessment of effective 'gene expression age' under axenic conditions (Figure 1D) are now seen to become uncoupled from age in the absence of a bacterial microbiome, we reinvestigated the calculation of transcriptomic aging rate based on gene expression profiling. Rather than performing age assessment using the complete set of genes that are age-correlated

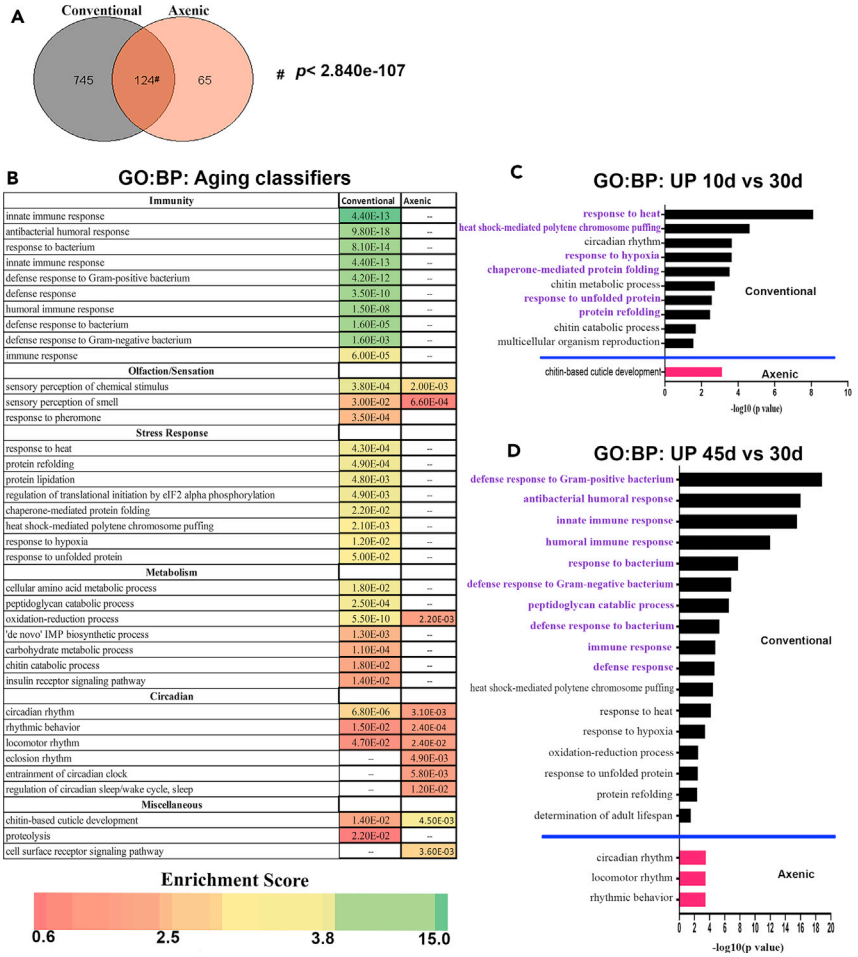

Immunity	Conventional	Axenic
innate immune response	4.40E-13	--
antibacterial humoral response	9.80E-18	--
response to bacterium	8.10E-14	--
innate immune response	4.40E-13	--
defense response to Gram-positive bacterium	4.20E-12	--
defense response	3.50E-10	--
humoral immune response	1.50E-08	--
defense response to bacterium	1.60E-05	--
defense response to Gram-negative bacterium	1.60E-03	--
immune response	6.00E-05	--
Olfaction/Sensation		
sensory perception of chemical stimulus	3.80E-04	2.00E-03
sensory perception of smell	3.00E-02	6.60E-04
response to pheromone	3.50E-04	
Stress Response		
response to heat	4.30E-04	--
protein refolding	4.90E-04	--
protein lipidation	4.80E-03	--
regulation of translational initiation by eIF2 alpha phosphorylation	4.90E-03	--
chaperone-mediated protein folding	2.20E-02	--
heat shock-mediated polytene chromosome puffing	2.10E-03	--
response to hypoxia	1.20E-02	--
response to unfolded protein	5.00E-02	--
Metabolism		
cellular amino acid metabolic process	1.80E-02	--
peptidoglycan catabolic process	2.50E-04	--
oxidation-reduction process	5.50E-10	2.20E-03
'de novo' IMP biosynthetic process	1.30E-03	--
carbohydrate metabolic process	1.10E-04	--
chitin catabolic process	1.80E-02	--
insulin receptor signaling pathway	1.40E-02	--
Circadian		
circadian rhythm	6.80E-06	3.10E-03
rhythmic behavior	1.50E-02	2.40E-04
locomotor rhythm	4.70E-02	2.40E-02
eclosion rhythm	--	4.90E-03
entrainment of circadian clock	--	5.80E-03
regulation of circadian sleep/wake cycle, sleep	--	1.20E-02
Miscellaneous		
chitin-based cuticle development	1.40E-02	4.50E-03
proteolysis	2.20E-02	--
cell surface receptor signaling pathway	--	3.60E-03

Figure 4. Gene ontology analysis of aging classifier genes and comparison of conventional *vs* axenic conditions

(A) Venn diagram showing the number of aging classifiers common between conventional flies (black circle) and axenic (orange circle). Significance assessed by a hypergeometric distribution test: http://nemates.org/MA/progs/overlap_stats.html. For this figure, classifiers for the conventional condition were selected based only on data from 10-, 30-, and 45-day data to facilitate comparison to the axenic data.

(B) Comparison of significantly enriched gene ontology (GO) groups for biological processes (BP) in aging classifier gene lists from conventionally-raised vs axenic-raised flies. Full list of classifier genes is in Table S8, and genes that belong to individual biological processes is in Table S9. Heatmap is based on DAVID enrichment scores and value in each cell is the pvalue calculated by DAVID; cells marked with '—' were not enriched)

(C) Significantly enriched ($p \leq 0.05$), biological process terms for genes upregulated in 10-day-old conventional (black bars) and axenic (red bar) raised flies, each compared to its respective 30-day-old condition. Biological processes related to stress response are highlighted in purple. Full list of genes used for analysis is in Table S10 and genes that belong to individual biological processes is in Table S11.

(D) Significantly enriched ($p \leq 0.05$) biological process terms for genes upregulated in 45-day-old conventional (black bars) and axenic (red bars) raised flies, each compared to its respective 30-day-old condition. Biological processes related to immunity are highlighted in purple. Full list of genes used for analysis is in Table S10 and genes that belong to individual biological processes is in Table S11.

See also Figure S7.

under conventional conditions, we limited the age calculation to those genes that are shared between the list of aging classifiers selected under conventional conditions and those selected under axenic conditions (124 genes, Table S12). Specifically, this list of shared classifiers was used to construct an age model using gene expression data from conventional flies, and that model was then applied to expression data from axenic flies. We now found that the slope of calculated age vs chronological age, i.e., the effective rate of transcriptional aging, for axenic flies is reduced only modestly, though significantly, in axenic flies from that in conventionally raised flies (26.3% reduction in slope; $p = 0.0002$; $F = 18.29$, DFd = 30; Figure 5).

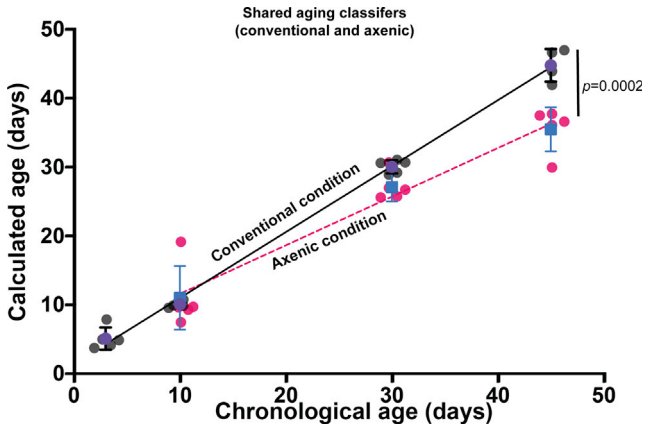

Figure 5. Comparison of transcriptomic aging rate in conventional vs axenic conditions

Age-classifier genes selected separately in conventional or axenic conditions were compared and shared classifiers were identified. A linear model for transcriptomic age (calculated age) was developed from gene expression data of conventionally raised flies using the shared classifiers, and this model was applied to calculate the effective transcriptomic age of axenic flies. Conventional samples: replicates are gray circles; mean value is a purple circle; SD as indicated. Axenic samples: replicates are red circles; mean value is a blue square; SD as indicated. Black line is the regression line for calculated vs chronological age for conventionally raised samples; dashed red line is the regression line for axenic samples. The significance of the difference in slope was calculated with GraphPad Prism using linear regression analysis. The full list of shared aging classifier genes is in Table S12.

This is consistent with the modest increase in lifespan observed under axenic conditions (12% and 20% increase in median and maximum lifespan, respectively; Figures 1A and 1B). Stated otherwise, the surprisingly flat slope of the transcriptomic aging curve in the axenic state (Figure 1D) does not arise primarily from a decrease in the rate of change of age-correlated biomarkers, but rather from a massive change in the composition of which processes are age-correlated.

Physiological tests reinforce results from expression profiling of axenic flies

Given the surprising pattern of results from gene expression profiling of axenic flies, it was essential to test those results and assess their implications through direct physiological assays. We first investigated the response of these flies to different biotic and abiotic stresses at various ages. We analyzed sensitivity to oxidative stress for 10d-, 30d-, and 45d-old conventional and axenic flies by measuring their survival when fed with 5% H_2O_2. We observed that 10d- and 45d-old axenic flies resisted oxidative stress significantly better than conventionally raised flies ($p < 0.0001$ for 10d-old conventional vs axenic; $p < 0.0001$ for 45d-old conventional vs. axenic; Figure 6A; Table S13), even though their initial, baseline expression of stress response genes was significantly lower than that of flies raised under conventional, microbe-rich conditions, particularly at 10 d. In contrast, tolerance of oxidative stress by 30d-old flies was the same irrespective of the presence or absence of bacteria ($p = 0.2123$), consistent with the nearly identical expression profiles of 30 d conventionally raised and axenic flies. Next, we examined the survival of 10d-, 30d- and 45d-old conventional and axenic flies under starvation conditions. Much as for oxidative stress, axenic flies at 10d- and 45d-of age also survive starvation stress longer than conventionally raised flies ($p < 0.0001$ for 10-day-old conventional vs. axenic; $p < 0.0001$ for 45d-old conventional vs. axenic; Figure 6B; Table S13), while the survival of 30d-old flies was not affected by presence vs absence of bacteria ($p = 0.1889$).

We next compared the resistance of axenic vs conventionally raised flies to microbial challenge, in light of the failure of axenic flies to induce age-dependent activation of the innate immune response. We pricked appropriately aged flies with lancets dipped in an active culture of the *Drosophila* pathogen *Erwinia carotovora subsp. carotovora* (ATCC 15390) or performed sterile pricking as a control. We found that axenic flies tested at 10-day- and 30-day-old resisted microbial challenge significantly better than conventional flies ($p < 0.0001$). We note that these times of challenge are prior to the onset of most of the age-dependent increase in expression of innate immunity genes that occurs under conventional conditions. In contrast, 45-day-old axenic flies succumbed substantially earlier upon infection than did conventionally raised 45-day-old flies that had already induced high-level expression of antimicrobial proteins prior to challenge ($p <$

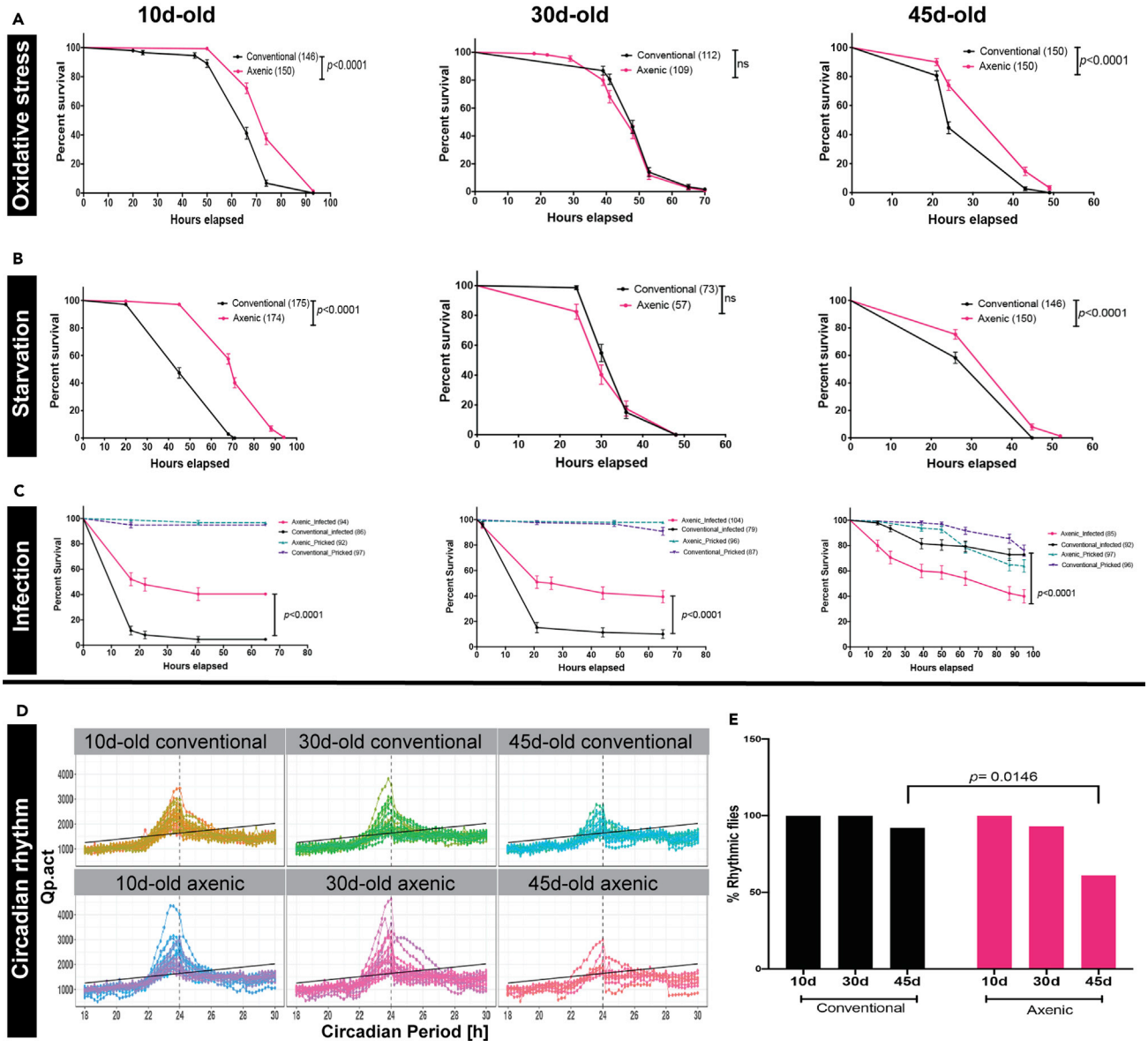

Figure 6. Effect of axenic growth on measures of host physiology

Mated male flies were raised in parallel to the indicated ages under either conventional or axenic conditions. They were then subjected to the indicated stressor and percent survival was assayed at the times of treatment shown. In all graphs, black line is a survivorship curve post-treatment for conventionally raised flies and red is for axenic. Plotted values are mean ± SEM; pvalues are indicated (Mantel-cox logrank test) and number of flies used is indicated in parentheses. ns denotes "not significant ($p > 0.05$).

(A–C)(A) Hydrogen peroxide (H_2O_2, 5%), Survival curve shows data pooled from 5-6 biological replicates (B) Starvation conditions. Survival curve was generated using five biological replicates (C) Pathogen challenge. Flies were pricked in the thorax with a needle dipped in an active culture of the *Erwinia carotovora subsp. carotovora* or with a sterile control. Fifty flies were infected for each age and condition, however, only those that survived the pricking were scored further. Control survivorship curves: dotted purple line for sterile pricking of conventionally raised flies; dotted cyan line for sterile pricking of axenic flies. Raw survival data per vial is provided in Table S13.

(D)χ^2 periodogram of rhythmic flies. Wild type conventionally-raised or axenic flies of the indicated ages entrained to 12:12 light:dark cycle were put in constant dark, and activity was monitored for 8 days. Within each panel, each line shows the correlation of activity with circadian period (Qp) for one fly over a range of potential periods (18–30 hr; χ^2). The peak of the curve is taken to indicate the circadian period for that individual. n = 32 flies for each condition were set up.

(E) Fraction of flies of the indicated age and microbial status showing statistically significant rhythmic behavior, based on the periodogram. Percentage of rhythmic flies was calculated based only on those that survived the entire experiment. Significance calculated by Fisher's Exact Test.

See also Figures S8–S10.

0.0001; Figure 6C; Table S13). Consistent with these observations, we find that AMP upregulation 16 hr after pathogen challenge at 10d-old is approximately equivalent in conventionally-raised and axenic flies (Figure S8), but that the introduced bacteria grow to ~4x higher density in the conventionally raised flies, consistent with their higher rate of mortality. A possible rationale for this observation will be presented in the Discussion. Taken together, these data correlate well with the gene expression data and illuminate the physiological consequences of the differences in gene expression between conventional- and axenic-grown flies.

In contrast to the processes above, Rhythmic Behavior was a major GO category that showed substantial age-dependence both in the presence and absence of a bacterial microbiome (Figure 4B). Therefore, we examined circadian rhythm in both conventional and axenic flies at 10d, 30d, and 45d of age. Consistent with the GO analysis, circadian rhythm degrades with age in both conventional and axenic flies. However, the absence of bacteria significantly enhances the effect of age on circadian rhythm in older flies (Figure 6D). We found that 92% of 45-day-old conventionally raised flies maintain rhythmic behavior after 8 d of constant darkness, while only 61% of axenic flies were able to do so (Figure 6E, $p = 0.0146$). Moreover, whereas 45-day conventionally-grown flies that maintained rhythmicity in the dark showed circadian periods closely clustered around 24 hr, those 45-day axenic flies that did maintain rhythmicity displayed periods ranging from 18.8 to 25.8 hr ($p = 0.0001$; F-test for variance). These data show that circadian rhythm remains age-dependent in axenic conditions, as it is in normal flies, consistent with the expression profiling analysis, but it also reveals an important role for the microbiota in the maintenance of circadian rhythm in old age.

Removing the microbiome-dependent contribution to age-correlated genes identifies candidates for processes that may be autonomously time-dependent

Axenic flies live somewhat longer than conventionally grown flies, and linear modeling using aging classifiers shared between conventionally grown and axenic flies reveals that the rate of change of age-correlated biomarkers is broadly similar in the two growth conditions, decelerating only modestly in the axenic state. This suggests a strong commonality in at least some of the ways that the transcriptome changes over adulthood with and without a bacterial microbiome, despite the massive differences in gene expression profiles in the two conditions. It further suggests that analysis of the axenic aging profile can reveal processes that are independent of the bacterial microbiome, and that also change with age in the conventionally grown population. To test this hypothesis, we first asked whether the aging classifier genes derived solely from the axenic expression profiles (above, Figure 1D; Table S8) could generate an effective age prediction metric, as can genes from the conventional condition, and found that they did (calculated ages for 10-, 30-, and 45-day axenic flies: 10.7 ± 1.5; 29.9 ± 0.8; 44.1 ± 1.6; mean $\pm$ SEM; Figure 7A). As described above, GO analysis of the classifier genes derived from the axenic expression profiling dataset identifies rhythmic processes, cuticular maintenance, olfactory perception, and a subset of metabolic and redox processes (largely mitochondrial-associated processes; see Discussion) as major enriched categories (Figure 7B). This demonstrates that these biological processes are features of aging that are independent of the presence of a bacterial-rich environment, making them candidates for processes whose time-dependence could potentially be autonomous to the organism. Alternatively, it could be that the change over time of these processes is dependent on some other external influence that we have not investigated.

DISCUSSION

We have shown here that ~70% of the systematic changes in gene expression that normally occur over the course of adult aging in *Drosophila* do not happen if flies are grown under bacteria-free conditions. These include two "hallmarks of aging" (López-Otín et al., 2013) that are observed widely across most animal phyla, the decline in expression of stress-response genes over the earlier part of adult life and the activation of the innate immune response in the latter part of life (Dues et al., 2016; Zerofsky et al., 2005). Our data demonstrate, therefore, that these two processes are not inevitable features of aging, but rather reflect the sequential deployment by the organism of a series of strategies to respond to the challenges of its normal microbial environment. In contrast, even under bacteria-free conditions, we detect four major classes of age-dependent changes in gene expression that parallel those that occur under conventional, microbe-rich conditions. These, therefore, remain candidates for potentially being processes that are intrinsic to the progressive physiological decline of aging, though it remains to be seen whether they can be separated from aging by some other environmental manipulation. These time-dependent processes include olfaction/pheromone sensing, cuticular maintenance, circadian rhythm, and a subset of

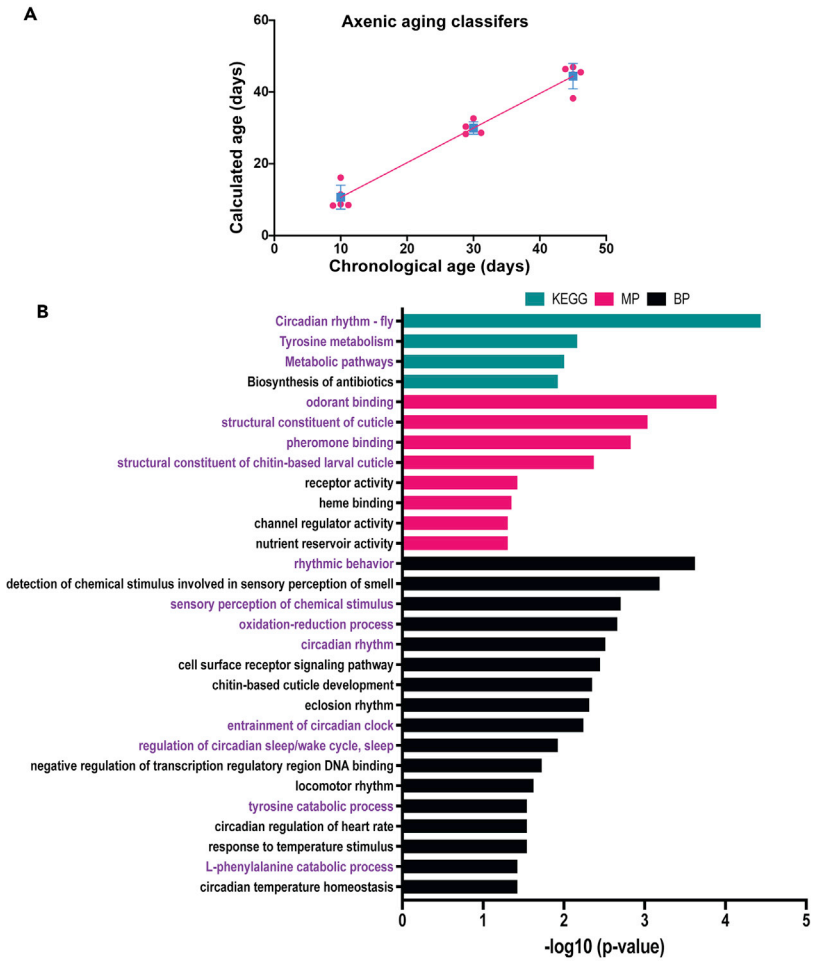

Figure 7. Expression analysis of axenic flies reveals aging processes that are independent of the bacterial microbiome

Gene expression data from axenic flies aged for 10d, 30d, and 45d were used to select aging classifier genes (189 genes). These were used to generate a linear model of calculated age for axenic flies (red line). n = five biological replicates for all samples. Red circles represent individual data points and blue square represents mean for axenic flies (SD indicated by blue line). (B) GO analysis of aging classifiers of axenic samples, using DAVID. Biological processes are the same as those shown in Figure 4B, however, this figure includes molecular function as well as KEGG pathway. GO processes related to metabolism, sensation, olfaction and circadian rhythm are highlighted in blue. X-axis represents -$\log_{10}$ of pvalue.
See also Figure S11.

metabolic processes, particularly mitochondrial-associated processes. In as much as all of these processes modulate lifespan, both those processes that are essentially a response to the bacterial microbiome and those that are not, these data underscore the idea that the coupling between the internal transcriptional state of the individual and lifespan is not fixed. Rather, lifespan integrates the effects of a series of separable processes, only some of which reflect autonomous changes in the internal state of the individual with time (Pletcher et al., 2000; Smith et al., 2020).

Initial application of an age metric calculated from all the age-classifier genes that are detected under conventional growth conditions gave the appearance that when flies are grown without a bacterial microbiome, the overall pattern of genome-wide gene expression fails to evolve with chronological age. A deeper analysis, however, revealed that this is not the case. Rather, more than 2/3 of the genes whose expression we think of as being associated with the process of aging, in fact, are only age-correlated because of the effects of the bacterial microbiome. Remarkably, this group includes some of the most extensively studied age-correlated GO categories, such as innate immune response (Fabian et al., 2018)

and stress response (Dues et al., 2016). When these microbiome-dependent genes are removed from consideration, and transcriptomic age is calculated using only classifier genes that are shared between the conventional and axenic states, we see that axenic growth causes only a mild deceleration of transcriptional aging (~26%), consistent with the modest, 12–20% extension of lifespan we observe under axenic conditions. The ~70% reduction in age-dependent variance in gene expression that we report under axenic conditions was observed using five different analyses of our data. A similar effect moreover is observed upon re-analysis of published data from another group (Broderick et al., 2014), in which we find that the number of age-dependent genes identified by microarray from the midgut of adult female flies was reduced by ~40% by axenic growth. All these analyses also agree in identifying stress response, innate immunity, and a subset of metabolic processes as the main age-correlated features that are dependent on the microbial environment and not directly on chronological age.

Our data show, unexpectedly, that some of the age-dependent changes in gene expression that are observed most commonly across phylogeny, and that are typically viewed as reflecting physiological deficits that are inherent to organismal aging, in fact, are not reflective simply of the passage of time, nor should they be considered deficits (de Magalhaes et al., 2009; López-Otín et al., 2013; McCarroll et al., 2004). Dynamic regulation of stress response genes and innate immune genes (McHugh et al., 2020) are revealed to be separate adaptations evolved to support life in a microbe-rich environment, but strategies that happen to be optimized for different stages in the lifecycle. Thus, in the young adult fly, the organism transiently upregulates its stress response genes, presumably to respond to the stress produced by its resident microbial population, but only if that microbial population is present, and damps down that expression as the fly ages and it is no longer required. Late in adulthood, the fly upregulates its innate immune system, presumably to limit the replicative growth of the microbiome, but again only if that microbiome is indeed present. Our results are in agreement with earlier reports showing that interventions that reduce microbial exposure also reduce age-related activation of the immune response (Clark and Walker, 2018; Guo et al., 2014; Ren et al., 2007). Thus, high-level expression of stress genes early and their decline with time are not obligatory aspects of aging, and neither is the elevated expression of cytotoxic immune effectors at older ages. Each is a response that is actively induced by the presence of the bacterial microbiome, and each supports viability in the face of that microbiome, targeted especially to a particular portion of the lifecycle. This further reveals that the bacterial microbiome does not simply modulate individual details of aging, but rather that it is responsible for much of the overall architecture of age-dependent gene expression. A critical remaining question is whether the time-dependent switch in the nature of the fly's response to the microbiome arises from an internal change in the state of the host with age, whether it reflects the evolving ecology of the bacterial flora itself, or some combination of the two. Experiments to investigate this question are currently in progress.

It was surprising that young, conventionally raised flies showed greater sensitivity to acute oxidative or starvation stress than did axenic flies, despite their substantially higher baseline expression of stress-response genes prior to the challenge. One possible explanation is that the conventionally raised flies are already using much of their available stress response machinery to protect against the consequences of microbial colonization and therefore have limited capacity remaining to respond to additional, acute, environmental stress, whereas axenic flies have less of a chronic load and thus retain that spare capacity. The same is evidently true of pathogen challenge at a young age, as inoculation with equal amounts of bacteria leads to greater bacterial growth, and greater lethality, in young, conventionally raised flies than young axenic flies even though activation of antimicrobial peptide expression in response to the challenge is roughly equivalent in the two populations. It may be, for example, that other aspects of the immune response, such as phagocytes and crystal cells, are more effective at suppressing acute infection in young axenic flies as their capacity is not already depleted in responding to conventional flora. Other explanations are also possible, however, and further study will be required to determine this. In contrast, the old, conventionally raised fly had greater resistance to pathogen challenge than did the old axenic fly. Here, we imagine that survival of pathogen challenge late in life was enhanced by the pre-existing, high-level expression of AMPs (Table S5) that is a normal component of gene expression in later adulthood under conventional conditions but is lacking in the axenic state even at advanced chronological age.

Perhaps one of the most surprising observations from our analysis occurred at the middle of adulthood, ~30 days after adult eclosion, when gene expression was found to be nearly identical in the absence of bacterial flora to what it was in the presence, with only 0.4% of genes showing a statistically significant

difference in level. Evidently, at this stage, the animal's physiology is optimally adapted to life in its typical bacterial environment without the need for a further transcriptional response. Earlier than this, additional expression of stress-response genes is beneficial; after this, additional expression of innate immune effectors is beneficial. At 30 days, neither is required and in fact, the difference in stress and starvation sensitivity between axenic and normal flies goes away.

While there is a greatly reduced time-dependent change in gene expression under axenic conditions, significant changes in gene expression do still occur. Those changes, moreover, are largely consistent between conventional and axenic conditions, making these genes excellent biomarkers for the internal state of the animal as a function of age. Consistent with this, the central role of Olfactory Sensory Function in the regulation of lifespan is well established in both *Drosophila* and *C. elegans* (Apfeld and Kenyon, 1999; Libert and Pletcher, 2007), though a teleological explanation remains unclear. Similarly, the importance of Cuticular Integrity in aging has been studied extensively (Herndon et al., 2002; Kuo et al., 2012). In the fly, it has been linked to preventing desiccation (Nghiem et al., 2000), as well as, perhaps, modulating the formation and release of pheromones (Kuo et al., 2012) that interact with the olfactory machinery. Interpretation of age-dependent changes in expression of metabolic genes is less clear-cut, as these are split between those that are bacterial-dependent and those that are not. Examination of the gene lists suggests that many of the bacterial-independent Metabolic changes are in processes that are linked to mitochondria (27/54 metabolic categories, based on KEGG analysis of the polyserial gene list (Table S14), but this set of features is complex and untangling it will require additional investigation. Perhaps the most unexpected age-correlated feature is the regulation of circadian rhythm. Changes in circadian rhythmicity with age have been observed in a number of species, including humans as well as flies, and there is evidence for changes in circadian rhythm modifying lifespan, though evidence as to whether the altered rhythm is associated with increased or decreased lifespan remains inconsistent (Koh et al., 2006; Pandi-Perumal et al., 2002; Ulgherait et al., 2020). The identification of a bacterial-independent component of age-dependent change in gene expression, therefore, offers one step toward asking whether there exists a minimal set of processes whose change over the course of aging is linked inextricably to the passage of time, regardless of external influences. It will be important to test additional environmental manipulations to see which of the four processes identified here show altered variation over time in response to some other external variable(s) and which, if any, are autonomous to the individual.

The data presented here are all derived from *Drosophila*, but it seems likely that the underlying principles apply broadly throughout the animal kingdom. The outlines of the aging process are substantially conserved genetically, physiologically, and pharmacologically across the phylogeny of multicellular animals (Mitchell et al., 2015), and indeed, many features are found even in unicellular organisms, such as *Saccharomyces cerevisiae* (Liu and Acar, 2018). More specifically, the pattern of changes one observes in gene expression with age are highly conserved (Irizar et al., 2019), including those GO categories that we now see require the presence of the bacterial microbiome. This immediately raises the question of whether the pattern of dependence on the microbiome that we observe for gene expression in the fly will also be true in other animals, including humans. To begin to examine this possibility, we analyzed our data with gProfiler, which identifies human disease processes linked to the human orthologs of *Drosophila* genes (Reimand et al., 2007). We found that the aging classifiers from conventionally grown flies have human orthologs linked to a wide variety of pathologies of aging, including processes associated with muscular degeneration, skin barrier proliferation, peripheral nerve degeneration, and cataracts, among others (Figure S11). Strikingly, however, more than 90% of these human aging pathologies are linked to the orthologs of genes whose age-dependence in the fly is specific for growth in bacteria-rich, conventional conditions, and are absent from the list of aging classifiers identified in the axenic state (Figure S11). This raises the specter that the associated diseases of human aging may similarly be strongly linked to the status of the human microbiome and its associated immune response. It may be, therefore, that for humans, as for flies, net lifespan reflects the ticking both of a clock responding to the internal state of the animal, but also from parallel, independent clocks responding to various environmental challenges, particularly the microbiome.

Limitations of the study

- To control variance, only male flies were used in the experiment, and only head RNA was queried. In the future, it will be important to compare results in females, whose aging and microbiome differ

from those of males in significant ways. Analysis of other tissues will undoubtedly reveal additional correlates of aging.

- It was necessary to use antibiotics to maintain flies in a bacteria-free state for the full course of the experiment. Control experiments presented in the text argue strongly that the results as a whole reflect the absence of bacteria and not the presence of the antibiotic, but we cannot rule out effects of antibiotics on specific details of the data.
- It was not possible to prevent the presence of fungi in the bacteria-free flies. Data presented in the paper demonstrate that the total density of fungi is ~1.0% the density of bacteria under conventional conditions and that the fungal load is not increased when bacterial growth is suppressed with antibiotic, but we cannot rule out the possibility that an anti-fungal response makes some contribution to the aging data.

STAR★METHODS

Detailed methods are provided in the online version of this paper and include the following:

- KEY RESOURCES TABLE
- RESOURCE AVAILABILITY
  - Lead contact
  - Materials availability statement
  - Data and code availability
- EXPERIMENTAL MODEL AND SUBJECT DETAILS
- METHOD DETAILS
  - Lifespan assay
  - Microarray and mRNA expression analysis
  - Gene ontology analysis
  - qPCR validation
  - Removal of antibiotics from axenic flies
  - Acute generation of axenic flies without antibiotics
  - Stress sensitivity assay
  - Quantitative analysis of circadian rhythm
- QUANTIFICATION AND STATISTICAL ANALYSIS

SUPPLEMENTAL INFORMATION

Supplemental information can be found online at https://doi.org/10.1016/j.isci.2021.102703.

ACKNOWLEDGMENTS

We are grateful to all the members of our lab for helpful discussion during the performance of these experiments, and we especially thank Joy Gu and Irina Kuzina for outstanding technical assistance, and Andrew Wodrich for assistance preparing the Graphical Abstract. We also wish to thank Shailesh Kumar and Susan Harbison for advice and assistance with circadian rhythm experiments and for the use of their Activity Monitoring System; Ying Hu, Veronique Bolduc, and Carsten Bonnemann for the use of their qPCR machine; Ben White and Quan Yuan for use of their circadian-controlled fly room, and Abdel Elkahloun and the NHGRI Microarray Core Facility for generating the microarray data for our study. For insightful comments on the manuscript, we are grateful to Mark Cookson, Elaine Ostrander, Manish Mishra, Andrew Scott, Bryan Traynor, and Andrew Wodrich. This work was supported by the Basic Neuroscience Program of the Intramural Research Program of the NIH (NINDS): ZIA NS003106 to EG. KJ was supported by intramural funds of NINDS.

AUTHOR CONTRIBUTIONS

AKS: Conceptualization, Investigation, Formal Analysis, Writing, Visualization.

KJ: Methodology, Software, Formal Analysis, Data Curation, Visualization.

EG: Conceptualization, Writing, Supervision, Project Administration, Funding Acquisition.

DECLARATION OF INTERESTS

The authors declare no competing interests.

Received: January 29, 2021
Revised: April 30, 2021
Accepted: June 7, 2021
Published: July 23, 2021

REFERENCES

Apfeld, J., and Kenyon, C. (1999). Regulation of lifespan by sensory perception in Caenorhabditis elegans. Nature *402*, 804–809.

Belkaid, Y., and Hand, T.W. (2014). Role of the microbiota in immunity and inflammation. Cell *157*, 121–141.

Broderick, N.A., Buchon, N., and Lemaitre, B. (2014). Microbiota-induced changes in Drosophila melanogaster host gene expression and gut morphology. mBio *5*, e01117–01114.

Brummel, T., Ching, A., Seroude, L., Simon, A.F., and Benzer, S. (2004). Drosophila lifespan enhancement by exogenous bacteria. Proc. Natl. Acad. Sci.U S A *101*, 12974–12979.

Cichewicz, K., and Hirsh, J. (2018). ShinyR-DAM: a program analyzing Drosophila activity, sleep and circadian rhythms. Commun.Biol. *1*, 25.

Clark, I., Salazar, A., Yamada, R., Fitz-Gibbon, S., Morselli, M., Alcaraz, J., Rana, A., Rera, M., Pellegrini, M., Ja, William W., et al. (2015). Distinct shifts in microbiota composition during Drosophila aging impair intestinal function and drive mortality. Cell Rep. *12*, 1656–1667.

Clark, R.I., and Walker, D.W. (2018). Role of gut microbiota in aging-related health decline: insights from invertebrate models. Cell. Mol. Life Sci. *75*, 93–101.

de Magalhaes, J.P., Curado, J., and Church, G.M. (2009). Meta-analysis of age-related gene expression profiles identifies common signatures of aging. Bioinformatics *25*, 875–881.

Dudoit, S., Fridlyand, J., and Speed, T.P. (2002). Comparison of discrimination methods for the classification of tumors using gene expression data. J. Am. Stat. Assoc. *97*, 77–87.

Dues, D.J., Andrews, E.K., Schaar, C.E., Bergsma, A.L., Senchuk, M.M., and Van Raamsdonk, J.M. (2016). Aging causes decreased resistance to multiple stresses and a failure to activate specific stress response pathways. Aging *8*, 777–795.

Fabian, D.K., Garschall, K., Klepsatel, P., Santos-Matos, G., Sucena, É., Kapun, M., Lemaitre, B., Schlötterer, C., Arking, R., and Flatt, T. (2018). Evolution of longevity improves immunity in Drosophila. Evol.Lett. *2*, 567–579.

Fraga, C.G., Shigenaga, M.K., Park, J.W., Degan, P., and Ames, B.N. (1990). Oxidative damage to DNA during aging: 8-hydroxy-2'-deoxyguanosine in rat organ DNA and urine. Proc. Natl. Acad. Sci.U S A *87*, 4533–4537.

Fushan, A.A., Turanov, A.A., Lee, S.G., Kim, E.B., Lobanov, A.V., Yim, S.H., Buffenstein, R., Lee, S.R., Chang, K.T., Rhee, H., et al. (2015). Gene expression defines natural changes in mammalian lifespan. Aging Cell *14*, 352–365.

Galenza, A., Hutchinson, J., Campbell, S.D., Hazes, B., and Foley, E. (2016). Glucose modulates Drosophila longevity and immunity independent of the microbiota. Biol. Open *5*, 165–173.

Gendrin, M., Welchman, D.P., Poidevin, M., Hervé, M., and Lemaitre, B. (2009). Long-range activation of systemic immunity through peptidoglycan diffusion in Drosophila. PLoS Pathog. *5*, e1000694.

Gould, A.L., Zhang, V., Lamberti, L., Jones, E.W., Obadia, B., Korasidis, N., Gavryushkin, A., Carlson, J.M., Beerenwinkel, N., and Ludington, W.B. (2018). Microbiome interactions shape host fitness. Proc. Natl. Acad. Sci.U S A *115*, E11951.

Guarente, L., and Kenyon, C. (2000). Genetic pathways that regulate ageing in model organisms. Nature *408*, 255–262.

Guo, L., Karpac, J., Tran, S.L., and Jasper, H. (2014). PGRP-SC2 promotes gut immune homeostasis to limit commensal dysbiosis and extend lifespan. Cell *156*, 109–122.

Han, B., Sivaramakrishnan, P., Lin, C.J., Neve, I.A.A., He, J., Tay, L.W.R., Sowa, J.N., Sizovs, A., Du, G., Wang, J., et al. (2017). Microbial genetic composition tunes host longevity. Cell *169*, 1249–1262 e1213.

Herndon, L.A., Schmeissner, P.J., Dudaronek, J.M., Brown, P.A., Listner, K.M., Sakano, Y., Paupard, M.C., Hall, D.H., and Driscoll, M. (2002). Stochastic and genetic factors influence tissue-specific decline in ageing C. elegans. Nature *419*, 808–814.

Hipp, M.S., Kasturi, P., and Hartl, F.U. (2019). The proteostasis network and its decline in ageing. Nat. Rev. Mol.Cell Biol. *20*, 421–435.

Hoban, A.E., Stilling, R.M., Ryan, F.J., Shanahan, F., Dinan, T.G., Claesson, M.J., Clarke, G., and Cryan, J.F. (2016). Regulation of prefrontal cortex myelination by the microbiota. Transl. Psychiatry *6*, e774.

Houthoofd, K., Braeckman, B.P., Lenaerts, I., Brys, K., De Vreese, A., Van Eygen, S., and Vanfleteren, J.R. (2002). Axenic growth up-regulates mass-specific metabolic rate, stress resistance, and extends life span in Caenorhabditis elegans. Exp. Gerontol. *37*, 1371–1378.

Huang, D.W., Sherman, B.T., and Lempicki, R.A. (2009a). Bioinformatics enrichment tools: paths toward the comprehensive functional analysis of large gene lists. Nucleic Acids Res. *37*, 1–13.

Huang, D.W., Sherman, B.T., and Lempicki, R.A. (2009b). Systematic and integrative analysis of large gene lists using DAVID bioinformatics resources. Nat. Protoc. *4*, 44–57.

Irizar, P.A., Schauble, S., Esser, D., Groth, M., Frahm, C., Priebe, S., Baumgart, M., Hartmann, N., Marthandan, S., Menzel, U., et al. (2019). Publisher Correction: transcriptomic alterations during ageing reflect the shift from cancer to degenerative diseases in the elderly. Nat. Commun. *10*, 2459.

Kirkwood, T.B., and Melov, S. (2011). On the programmed/non-programmed nature of ageing within the life history. Curr.Biol. *21*, R701–R707.

Koh, K., Evans, J.M., Hendricks, J.C., and Sehgal, A. (2006). A Drosophila model for age-associated changes in sleep:wake cycles. Proc. Natl. Acad. Sci.U S A *103*, 13843–13847.

Komljenovic A, L.H., Sorrentino, V., Kutalik, Z., Auwerx, J., and Robinson-Rechavi, M. (2019). Cross- species functional modules link proteostasis to human normal aging. PLoS Comput.Biol. *15*, e1007162.

Koyle, M.L., Veloz, M., Judd, A.M., Wong, A.C., Newell, P.D., Douglas, A.E., and Chaston, J.M. (2016). Rearing the fruit fly Drosophila melanogaster under axenic and gnotobiotic conditions. J. Vis.Exp. 54219.

Kuo, T.H., Yew, J.Y., Fedina, T.Y., Dreisewerd, K., Dierick, H.A., and Pletcher, S.D. (2012). Aging modulates cuticular hydrocarbons and sexual attractiveness in Drosophila melanogaster. J. Exp. Biol. *215*, 814–821.

Lee, H.-Y., Lee, S.-H., Lee, J.-H., Lee, W.-J., and Min, K.-J. (2019). The role of commensal microbes in the lifespan of Drosophila melanogaster. Aging *11*, 4611–4640.

Leftwich, P.T., Clarke, N.V.E., Hutchings, M.I., and Chapman, T. (2017). Gut microbiomes and reproductive isolation in Drosophila. Proc. Natl. Acad. Sci.U S A *114*, 12767–12772.

Leitao-Goncalves, R., Carvalho-Santos, Z., Francisco, A.P., Fioreze, G.T., Anjos, M., Baltazar, C., Elias, A.P., Itskov, P.M., Piper, M.D.W., and Ribeiro, C. (2017). Commensal bacteria and essential amino acids control food choice behavior and reproduction. PLoS Biol. *15*, e2000862.

Lesperance, D.N.A., and Broderick, N.A. (2020). Meta-analysis of diets used in Drosophila microbiome Research and introduction of the Drosophila dietary composition calculator (DDCC). G3 (Bethesda) *10*, 2207–2211.

Libert, S., and Pletcher, S.D. (2007). Modulation of longevity by environmental sensing. Cell *131*, 1231–1234.

Liu, P., and Acar, M. (2018). The generational scalability of single-cell replicative aging. Sci. Adv. *4*, eaao4666.

Livak, K.J., and Schmittgen, T.D. (2001). Analysis of relative gene expression data using real-time quantitative PCR and the 2(T)(-Delta Delta C) method. Methods *25*, 402–408.

López-Otín, C., Blasco, M.A., Partridge, L., Serrano, M., and Kroemer, G. (2013). The hallmarks of aging. Cell *153*, 1194–1217.

McCarroll, S.A., Murphy, C.T., Zou, S., Pletcher, S.D., Chin, C.S., Jan, Y.N., Kenyon, C., Bargmann, C.I., and Li, H. (2004). Comparing genomic expression patterns across species identifies shared transcriptional profile in aging. Nat. Genet. *36*, 197–204.

McHugh, D.R., Koumis, E., Jacob, P., Goldfarb, J., Schlaubitz-Garcia, M., Bennani, S., Regan, P., Patel, P., and Youngman, M.J. (2020). DAF-16 and SMK-1 contribute to innate immunity during adulthood in Caenorhabditis elegans. G3 *10*, 1521.

Mitchell, S.J., Scheibye-Knudsen, M., Longo, D.L., and de Cabo, R. (2015). Animal models of aging Research: implications for human aging and age-related diseases. Annu. Rev. Anim. Biosci. *3*, 283–303.

Nghiem, D., Gibbs, A.G., Rose, M.R., and Bradley, T.J. (2000). Postponed aging and desiccation resistance in Drosophila melanogaster. Exp. Gerontol. *35*, 957–969.

Pacifico, R., MacMullen, C.M., Walkinshaw, E., Zhang, X., and Davis, R.L. (2018). Brain transcriptome changes in the aging Drosophila melanogaster accompany olfactory memory performance deficits. PLoS One *13*, e0209405.

Pandi-Perumal, S.R., Seils, L.K., Kayumov, L., Ralph, M.R., Lowe, A., Moller, H., and Swaab, D.F. (2002). Senescence, sleep, and circadian rhythms. Ageing Res. Rev. *1*, 559–604.

Petkau, K., Parsons, B.D., Duggal, A., and Foley, E. (2014). A deregulated intestinal cell cycle program disrupts tissue homeostasis without affecting longevity in Drosophila. J. Biol. Chem. *289*, 28719–28729.

Pitt, J.N., and Kaeberlein, M. (2015). Why is aging conserved and what can we do about it? PLoS Biol. *13*, e1002131.

Pletcher, S.D., Khazaeli, A.A., and Curtsinger, J.W. (2000). Why do life spans differ? Partitioning mean longevity differences in terms of age-specific mortality parameters. J. Gerontol.A Biol. Sci. Med. Sci. *55*, B381–B389.

Pletcher, S.D., Macdonald, S.J., Marguerie, R., Certa, U., Stearns, S.C., Goldstein, D.B., and Partridge, L. (2002). Genome-wide transcript profiles in aging and calorically restricted Drosophila melanogaster. Curr. Biol. *12*, 712–723.

Ponton, F., Chapuis, M.P., Pernice, M., Sword, G.A., and Simpson, S.J. (2011). Evaluation of potential reference genes for reverse transcription-qPCR studies of physiological responses in Drosophila melanogaster. J. Insect Physiol. *57*, 840–850.

Pryor, R., Norvaisas, P., Marinos, G., Best, L., Thingholm, L.B., Quintaneiro, L.M., De Haes, W., Esser, D., Waschina, S., Lujan, C., et al. (2019). Host-microbe-drug-nutrient screen identifies bacterial effectors of metformin therapy. Cell *178*, 1299–1312.e1229.

Reimand, J., Kull, M., Peterson, H., Hansen, J., and Vilo, J. (2007). g:Profiler—a web-based toolset for functional profiling of gene lists from large-scale experiments. Nucleic Acids Res. *35*, W193–W200.

Ren, C., Webster, P., Finkel, S.E., and Tower, J. (2007). Increased internal and external bacterial load during Drosophila aging without life-span trade-off. Cell Metab. *6*, 144–152.

Richardson, A.G., and Schadt, E.E. (2014). The role of macromolecular damage in aging and age-related disease. J. Gerontol.A Biol. Sci. Med. Sci. *69*, S28–S32.

Rubinsztein, David C., Mariño, G., and Kroemer, G. (2011). Autophagy Aging Cell *146*, 682–695.

Schneider, D.I., Ehrman, L., Engl, T., Kaltenpoth, M., Hua-Van, A., Le Rouzic, A., and Miller, W.J. (2019). Symbiont-driven male mating success in the neotropical Drosophila paulistorum superspecies. Behav.Genet. *49*, 83–98.

Shukla, A.K., Spurrier, J., Kuzina, I., and Giniger, E. (2019). Hyperactive innate immunity causes degeneration of dopamine neurons upon altering activity of Cdk5. Cell Rep. *26*, 131–144.e134.

Smith, P., Willemsen, D., Popkes, M., Metge, F., Gandiwa, E., Reichard, M., and Valenzano, D.R. (2017). Regulation of life span by the gut microbiota in the short-lived African turquoise killifish. Elife *6*, e27014.

Smith, S.M., Elliott, L.T., Alfaro-Almagro, F., McCarthy, P., Nichols, T.E., Douaud, G., and Miller, K.L. (2020). Brain aging comprises many modes of structural and functional change with distinct genetic and biophysical associations. Elife *9*, e52677.

Spurrier, J., Shukla, A.K., McLinden, K., Johnson, K., and Giniger, E. (2018). Altered expression of the Cdk5 activator-like protein, Cdk5α, causes neurodegeneration, in part by accelerating the rate of aging. Dis. Models Mech. *11*, dmm031161.

Storelli, G., Defaye, A., Erkosar, B., Hols, P., Royet, J., and Leulier, F. (2011). Lactobacillus plantarum promotes Drosophila systemic growth by modulating hormonal signals through TOR-dependent nutrient sensing. Cell Metab. *14*, 403–414.

Stroustrup, N., Anthony, W.E., Nash, Z.M., Gowda, V., Gomez, A., Lopez-Moyado, I.F., Apfeld, J., and Fontana, W. (2016). The temporal scaling of Caenorhabditis elegans ageing. Nature *530*, 103–107.

Tabula Muris, C. (2020). A single-cell transcriptomic atlas characterizes ageing tissues in the mouse. Nature *583*, 590–595.

Ulgherait, M., Chen, A., McAllister, S.F., Kim, H.X., Delventhal, R., Wayne, C.R., Garcia, C.J., Recinos, Y., Oliva, M., Canman, J.C., et al. (2020). Circadian regulation of mitochondrial uncoupling and lifespan. Nat. Commun. *11*, 1927.

Vijg, J., and Montagna, C. (2017). Genome instability and aging: cause or effect? Transl. Med. Aging *1*, 5–11.

Yamada, R., Deshpande, S.A., Bruce, K.D., Mak, E.M., and Ja, W.W. (2015). Microbes promote amino acid harvest to rescue undernutrition in Drosophila. Cell Rep. *10*, 865–872.

Zerofsky, M., Harel, E., Silverman, N., and Tatar, M. (2005). Aging of the innate immune response in Drosophila melanogaster. Aging Cell *4*, 103–108.

STAR★METHODS

KEY RESOURCES TABLE

REAGENT or RESOURCE	SOURCE	IDENTIFIER
Bacterial strain		
Erwinia carotovora subsp. carotovora	ATCC	Cat#15390
Chemicals		
Nutri-Fly® BF, 10 x 1L Packets	Genesee Scientific	Cat#: 66-112, N/A
Gibco™Penicillin-Streptomycin (10,000 U/mL)	Life technologies	Cat#: 15140-122, N/A
PowerUp™ SYBR Green Master Mix	Applied biosystems	Cat#: A25742, N/A
High capacity cDNA Reverse Transcription Kit	Applied biosystems	Cat#:4368814, N/A
OneTaq® Quick-Load® 2X Master Mix	NEW ENGLAND BioLabs Inc	Cat#: M0486L, N/A
TRIzol® reagent	Life technologies	Cat#:15596026, N/A
Sodium Acetate Solution (3 M), pH 5.2	ThermoFisher Scientific	Cat#: R1181, N/A
Affymetrix VeriQuest Probe qPCR Master Mix	Affymetrix, Inc.	Cat#75650, N/A
Hydrogen peroxide solution	Sigma-Aldrich	Cat#:H1009-100ML, N/A
MRS agar plate	Tecknova	Cat#:M1350, N/A
YPD agar plate	Tecknova	Cat#:Y1000, N/A
Difco™ Nutrient Agar	BD Diagnostics	Cat#:213000 Lot#:8305685;
Difco™ Nutrient Broth	BD Diagnostics	Cat#:234000 Lot#:89192108
Sodium hypochlorite	Clorox	N/A
Phosphate buffer saline (PBS)	KD Medical	Cat#: RGE-3200, N/A
Ethyl Alcohol	Acros Organics	Cat# 615090020, N/A
Deposited data		
Raw and analyzed data	This paper	GEO
R-code for KNN/LOO selection of classifier genes	This paper and Spurrier et al. (2018)	https://data.ninds.nih.gov
Experimental models: Organisms/strains		
D. melanogaster:Oregon R^{+} (w^{+})	Laboratory of E. Giniger (Spurrier et al., 2018)	N/A
Oligonucleotides		
Primer for 27F: 5′-AGAGTTTGATCMTGGCTCAG-3′	Lee et al. (2019)	N/A
Primer for 1492R: 5′ TACGGYTACCTTGTTACGACTT 3′	Lee et al. (2019)	N/A
Probes for qPCR validation (Table S15)	This paper	N/A
Primers for Antimicrobial peptides (Table S15)	Shukla et al. (2019)	N/A
Software and algorithms		
Transcriptome Analysis Console (TAC) Software	ThermoFisher Scientific	https://www.thermofisher.com/us/en/home/life-science/microarray-analysis/microarray-analysis-instruments-software-services/microarray-analysis-software/affymetrix-transcriptome-analysis-console-software.html
R Project for Statistical Computing	The R project	http://www.r-project.org/ RRID:SCR_001905
Affymetrix GeneChip®Operating Software (GCOS)	Affymetrix	http://tools.thermofisher.com/content/sfs/brochures/gcos_datasheet.pdf

(*Continued on next page*)

Continued

REAGENT or RESOURCE	SOURCE	IDENTIFIER
ShinyR-DAM	Cichewicz and Hirsh (2018)	https://karolcichewicz.shinyapps.io/shinyr-dam/
GraphPad Prism 8.0	GraphPad	http://www.graphpad.com/ RRID:SCR_002798
DAVID version 6.8	Huang et al. (2009a), (2009b)	http://david.abcc.ncifcrf.gov
gProfiler	Reimand et al. (2007)	https://biit.cs.ut.ee/gprofiler/gost
Critical commercial assays		
GeneChip™Drosophila (melanogaster) Gene 1.0 ST Array	ThermoFisher Scientific	Cat#: 902155, N/A
Drosophila Activity Monitoring System	Trikinetics	https://trikinetics.com

RESOURCE AVAILABILITY

Lead contact

All requests for reagent and resources should be directed to the Lead Contact, Dr. Edward Giniger (ginigere@ninds.nih.gov).

Materials availability statement

This study did not generate new unique reagents.

Data and code availability

Numerical data for all figures is included in the Supplementary Tables. Microarray data is available on GEO (accession GSE174854). R-code for KNN/LOO selection of classifier genes has been published previously (Spurrier et al., 2018) and is available on the NIH public server (https://data.ninds.nih.gov/).

EXPERIMENTAL MODEL AND SUBJECT DETAILS

All the experiments were conducted using male Oregon Red (w^+), strain of Drosophila melanogaster. Fly stocks were maintained at 25°C, 50% humidity with 12:12 h light/dark cycle on the Bloomington Formulation (Nutri-Fly BF). Detailed data on the nutrient composition of this media can be found on the Fly Microbiome Diet Database (https://figshare.com/articles/dataset/Fly_Microbiome_Diet_Database/11920788(Lesperance and Broderick, 2020). Live yeast was not present in the food. Axenic flies were generated as described previously (Shukla et al., 2019). In brief, axenic flies were generated using embryos collected from overnight egg-laying on grape plates. Embryos were rinsed with 1X PBS and washed with 70% ethanol followed by dechorionation using 3% sodium hypochlorite for 7 min. Dechorionated embryos were rinsed with sterile water and transferred to sterile fly food supplemented with propionic acid (0.48ml/100ml) and Penicillin/Streptomycin (Pen Strep) at 1ml/100ml concentration. The embryos were cultured at 25°C and axenic conditions were confirmed by plating fly homogenate on Luria-Bertani medium and MRS agar plates as well as by 16S rDNA PCR using the universal primer. PCR reaction and thermocycler program as follow: Reaction mixture: OneTaq. Quick-Load master mix, template DNA, and Nuclease-free water. PCR Program: 94°C for 10 min, 94°C for 30s, 58°C for 30s, 72°C for 40s, 30 total amplification cycles, 72°C for 10 min, then hold 4°C. Axenic and conventional flies were raised on the same food for multiple generations to reduce heterogeneity arising due to diet. Sources of fly stocks, primer sequence and material used are provided as Key Resource Table.

METHOD DETAILS

Lifespan assay

The lifespan of conventional and axenic male flies was measured at 25°C under constant humidity with a 12:12 h light/dark cycle on the Bloomington Formulation (Nutri-Fly BF). Newly eclosed flies were allowed to mate for 3 d, then males were isolated and transferred to fresh vials (25/vial). To minimize the effect of CO2 anesthesia and separation-induced mortality, flies that died in the first 24h were excluded from the lifespan assay. Twenty-five flies were placed in each vial and flies were transferred to fresh vials and survival was scored twice a week. Graph Pad Prism 8.0 was used to determine Log-rank (Mantel-Cox) test for

statistical significance, and median survival. Significance of median survival was determined using the Mann-Whitney test.

Microarray and mRNA expression analysis

Microarray and mRNA expression analysis. All the microarray experiment and data analysis was done as per our earlier publication (Spurrier et al., 2018) using only heads from five biological replicates (each consisting of 50 male flies) for both growth conditions and each time point. Since this experiment was performed using only heads, we do not expect to see body specific effects such as expression changes selective for midgut. A detailed experimental description is as follows: Mated male flies were raised together to achieve the required age, collected and flash-frozen using liquid nitrogen and stored at -80°C. Once flies for all aging conditions were collected, total RNA was extracted from head samples using TRIzol. RNA was purified using 0.3M sodium acetate final concentration and ethanol. Purified RNA was processed and labeled according to the manufacturer's guidelines for use with the DroGene 1.0 ST GeneChip (Affymetrix, GeneChip Whole Transcript Sense Target Labeling). The Scanner 3000 (Affymetrix) was used along with the GeneChip Operation Software to generate one .CEL file per hybridized cRNA. These .CEL files were then imported into the Transcriptome Analysis Console and the Console was used to generate robust multi array average (RMA) normalized expression values per gene probe per imported file. This expression was then exported from the Console and imported into R for analysis. Quality of data was assessed and confirmed via Tukey box plot, covariance-based PCA scatter plot, and correlation-based heat map. To remove noise-biased expression, the mean and Coefficient of Variation (CV) per gene probe per sample class was calculated. Lowess was then used to model CV by mean expression per sample class producing one fit per sample class. These fits were then over-plotted to identify the common low-end expression value where the linear relationship between mean expression (signal) and CV (noise) was grossly lost (mean expression value=4.0). Expression values less than this value were floored to this value, while gene probes not having at least one sample greater than this value were discarded as non-informative. Annotations for gene probes not discarded were obtained from NetAffx (Affymetrix) and FlyBase (www.flybase.org). Expression per gene probe was tested for linear correlation with age and separately tested for differential expression across sample classes.

To test for linear correlation with age, polyserial correlation was used under a leave-one-out condition (library=polycor). Specifically, with each sample drop, we used polyserial correlation to generate a rho per gene testing the observed expression vs age under non-randomized condition and randomized condition. Z-scores were then calculated for each rho generated under non-randomized condition using the mean and SD of the rho estimates generated under randomized condition. P-values corresponding with these scores were then corrected using the Benjamini-Hochberg procedure. We considered genes as age markers if they had a corrected $P < 0.05$ under leave-one-out condition 100% of the time and were similarly significant under no leave-out-condition.

To test for differential expression across sample classes, the one-way analysis of variance (ANOVA) test was applied (Type III, library=car) using sample class as the factor under Benjamini–Hochberg false discovery rate multiple comparison correction (MCC) condition (library=multtest). Probes observed to have a corrected $P < 0.05$ by this test were deemed to have differential expression across the sample classes and further post hoc tested via Tukey's Honest Significance Difference (HSD) to identify which sample class comparisons probe expression was significantly different (post hoc $p<0.05$ and an absolute difference of means >1.5-fold). To determine which of the differential probes identified can robustly classify age, leave-one-out (LOO) testing was employed using the same method described earlier (Spurrier et al., 2018). For each LOO round, gene probes identified to have differential expression for at least one sample class comparison were used to construct a k-nearest neighbor (k-NN) model and predict the class of the left-out sample (Dudoit et al., 2002). Gene probes selected 100% of the time over all LOO rounds were deemed to be robust classifiers of age. These probes were then used to construct a principal component seeded AIC-optimized linear model using expression for day 3, 10, 30 and 45 control samples only. This model was then used to predict the physiological age of each biological replicate. Statistical differences in the predictions produced by the model were tested using the one-way ANOVA again (Type III) under MCC condition followed by Tukey's HSD test.

The same k-NN/LOO method was used to select age-classifier genes from the axenic samples, but using only day 10, 30, and 45 axenic samples, and for comparison, the method was re-applied to control samples, but limited to day 10, 30, and 45, as specified in the text.

Gene ontology analysis

Gene ontology analysis was performed for aging classifier genes using DAVID version 6.8 (Huang et al., 2009a, 2009b). The background was set to 'Drosophila_2 Array', and then 'Functional Annotation chart' with medium classification stringency. Significantly enriched GOTERM_BP_DIRECT categories were then selected manually from all other DAVID output. A non-log scale P-value less than 0.05 was considered statistically significant. The resulting annotated biological processes were grouped manually based on function and arranged by enrichment score as calculated by DAVID.

GO analysis to identify human disease processes linked to the human orthologs of Drosophila genes was done using gProfiler (Reimand et al., 2007). Statistical domain scope to only annotated genes, Benjamini-Hochberg FDR, and user threshold 0.05 were used as analysis conditions.

qPCR validation

Excess RNA from the microarray samples was converted into cDNA using the Applied Biosystems High-Capacity cDNA Reverse Transcription kit. Five biological replicates were run for every gene probe using the Affymetrix VeriQuest Probe qPCR Master Mix with specific TaqMan gene primers. qPCR reactions were prepared using the Affymetrix VeriQuest Probe qPCR Master Mix with specific TaqMan gene primers (Table S15); reactions were carried out on the QuantStudio 6 Real-Time PCR Systems using default settings. Threshold cycle numbers were determined automatically by the Applied Biosystems software. The set of probes included Rpl32 as a reference gene, which was used for normalization. Utility of Rpl32 as a reference was validated previously by analysis of expression level across the lifespan, and by comparison to the mean values of four commonly used *Drosophila* qRT-PCR reference genes (Ponton et al., 2011; Spurrier et al., 2018). Fold changes were determined using ΔΔCt (Livak and Schmittgen, 2001), relative to 10-d axenic.

Removal of antibiotics from axenic flies

To discriminate the effects of antibiotics vs microbiome on the expression profile in the axenic state, we raised axenic flies for 5 d on antibiotic containing food, then aseptically transferred the axenic flies to sterile food without antibiotic in the laminar hood and grew these flies an additional five days without antibiotic, flipping once to new food. In parallel, 5-day-old axenic flies were transferred to food vials that had previously been contaminated with normal *Drosophila* flora by being used to transiently culture conventionally raised flies. These flies were also grown for five days, flipping once to new, contaminated vials. The absence of bacteria in flies raised on non-antibiotic food, and its presence in flies restored to microbe-contaminated food, was verified by PCR (Figure S9). Finally, 10-day-old flies were frozen using liquid nitrogen, and qPCR was performed using RNA from head samples and probes listed in Table S15.

Acute generation of axenic flies without antibiotics

Embryos were bleached and transferred to sterile vials (twenty-five embryos per vial) either without or with antibiotics, respectively. After five days of fly emergence, flies from sterile vials were transferred either to fresh, sterile vials or to vials that had been used to house flies that had emerged from unbleached embryos and raised for an additional five days. Finally, 10-day-old, male flies were frozen and individual vials were examined for presence or absence of bacteria using 16S rDNA PCR (Figure S10). After verification of microbe-free and microbe-contaminated conditions, RNA from head samples was used to perform qPCR using probes listed in Table S15.

Stress sensitivity assay

Sensitivity to oxidative stress was assayed by survival following challenge with hydrogen peroxide (H_2O_2; 5%) as described earlier (Spurrier et al., 2018). Male flies at appropriate ages (10d, 30d and 45d) were starved for 3 hr on filter paper soaked with water and then transferred to vials having filter paper soaked with H_2O_2 with 5% sucrose. A parallel set of vials having sucrose only was used as control. For starvation sensitivity, flies were starved on water-soaked filter paper and survival was scored twice per day. Bacterial infections were performed by pricking adult flies with a lancet previously dipped into a concentrated culture (OD600=200) of the *Erwinia carotovora carotovora* (Gendrin et al., 2009). The parallel aseptic injury was used as a control for the infection experiment.

To examine whether axenic flies retain their ability to induce immune response genes and whether they tolerate or kill injected ECC15, 10-day-old flies were infected as described above. After 16 h of infection,

surviving flies were divided into two groups. One group was used for the assessment of internal bacterial load following a published protocol (Leitao-Goncalves et al., 2017), and another was used for qPCR of AMPs according to our earlier publication (Shukla et al., 2019).

Quantitative analysis of circadian rhythm

We recorded eight continuous days of activity in constant darkness (DD) using the Drosophila Activity Monitoring System. Activity counts were sampled in 1-min intervals. 32 flies were used in each condition of growth and age. ShinyR-DAM (Cichewicz and Hirsh, 2018) was used for data analysis.

QUANTIFICATION AND STATISTICAL ANALYSIS

GraphPad Prism 8.0 and R was used for data analysis. Statistical differences in survival curves (lifespan, oxidative stress response, and survival against bacterial infection) were measured by log rank (Mantel-Cox).

All statistical tests performed for this manuscript are specified in the text and figure legends. Sample randomization and blinding were not relevant and formal power analysis was not performed prior to initiating the study. Data from individual flies that suffered trauma from handling was censored from the analysis as specified in the Methods. One expression profiling sample was an outlier in the initial QC survey and was excluded from further analysis.